CHAPTER FIVE

Natural Isotope Abundance in Metabolites: Techniques and Kinetic Isotope Effect Measurement in Plant, Animal, and Human Tissues

Illa Tea[*,†,‡], **Guillaume Tcherkez**[*,1]

[*]Research School of Biology, Australian National University, Canberra, ACT, Australia
[†]Cancer Metabolism and Genetics Group, John Curtin School of Medical Research, Australian National University, Canberra, ACT, Australia
[‡]EBSI Team, CEISAM, University of Nantes-CNRS UMR 6230, Nantes, France
[1]Corresponding author: e-mail address: guillaume.tcherkez@anu.edu.au

Contents

Methods in Enzymology, Volume 596
ISSN 0076-6879
http://dx.doi.org/10.1016/bs.mie.2017.07.020

Abstract

The natural isotope abundance in bulk organic matter or tissues is not a sufficient base to investigate physiological properties, biosynthetic mechanisms, and nutrition sources of biological systems. In fact, isotope effects in metabolism lead to a heterogeneous distribution of ^{2}H, ^{18}O, ^{13}C, and ^{15}N isotopes in metabolites. Therefore, compound-specific isotopic analysis (CSIA) is crucial to biological and medical applications of stable isotopes. Here, we review methods to implement CSIA for ^{15}N and ^{13}C from plant, animal, and human samples and discuss technical solutions that have been used for the conversion to CO_2 and N_2 for IRMS analysis, derivatization and isotope effect measurements. It appears that despite the flexibility of instruments used for CSIA, there is no universal method simply because the chemical nature of metabolites of interest varies considerably. Also, CSIA methods are often limited by isotope effects in sample preparation or the addition of atoms from the derivatizing reagents, and this implies that corrections must be made to calculate a proper δ-value. Therefore, CSIA has an enormous potential for biomedical applications, but its utilization requires precautions for its successful application.

1. INTRODUCTION

Compound-specific stable isotope analysis by ratio mass spectrometry (CSIA) enables precise measurement of naturally occurring stable isotopes (such as $^{13}C/^{12}C$, $^{15}N/^{14}N$, $^{2}H/^{1}H$, $^{18}O/^{17}O$) within metabolites from complex mixtures (e.g., biological extracts). Isotopes are quantified using the isotope composition or δ-value (usually expressed in per mil):

$$\delta = \frac{R}{R_{st}} - 1$$

where R is the isotope ratio heavy/light ($^{13}C/^{12}C$, $^{15}N/^{14}N$, etc.) of the sample (metabolite) of interest, and R_{st} that in the international reference (Pee Dee Belemnite for ^{13}C, atmospheric N_2 for ^{15}N, standard mean oceanic water for ^{2}H and ^{18}O). δ-values provide a convenient tool to trace the origin and the fate of organic matter in a wide range of application such as environmental monitoring (Elsner & Imfeld, 2016), archeological studies (Styring et al., 2015), plant sciences (Aranjuelo, Cabrera-Bosquet, Mottaleb, Araus, & Nogués, 2009; de Rijke, Truyols, & de Koster, 2016; Dumont et al., 2013; González-Pérez, Jiménez-Morillo, de la Rosa, Almendros, & González-Vila, 2016; Hansen, Fromberg, & Frandsen (2014); Hettmann, Gleixner, & Juchelka, 2008; Lehmann, Gamarra, Kahmen, Siegwolf & Saurer, 2017; Mauve et al., 2016; Molero, Aranjuelo, Teixidor, Araus, & Nogués, 2011; Paolini, Ziller, Laursen,

Husted, & Camin, 2015; Styring, Fraser, Bogaard, & Evershed, 2014; Zech et al., 2013; Zhou et al., 2016), human and animal nutrition (Cantalapiedra-Hijar et al., 2016; Egli et al., 2016; Ferchaud-Roucher, Albert, Champ, & Krempf, 2006; Godin, Richelle, Metairon, & Fay, 2004; Godin et al., 2013; Morrison, O'Hara, King, & Preston, 2011; Petzke, Boeing, & Metges, 2005; Recio, Martín, Raposo, & Raposo, 2013; Reichardt, Barclay, Weaver, & Morrison, 2011; Styring et al., 2015; Tea, Ferchaud-Roucher, Küster, Darmaun, & Robins, 2007; Tea et al., 2013, 2016; Thevis, Piper, Horning, Juchelka, & Schänzer, 2013; Verbeke et al., 2010; Wang et al., 2014; Webb et al., 2015). Furthermore, the analysis of natural isotope abundance in different metabolites from the same extract, especially $^{13}C/^{12}C$ and $^{15}N/^{14}N$, can be used to investigate biosynthetic mechanisms and metabolic pathways in plant, animal, and human tissues. CSIA can also be implemented to enzymatic reaction assays allowing determination of kinetic isotope effects (KIEs) or equilibrium isotope effects (EIEs). Conversely, EIE and KIE are important pieces of information because they allow one to interpret isotope abundances in metabolites by taking into account enzymatic effects in metabolism.

In this chapter, we will focus on techniques for CSIA and associated KIE/EIE measurements and briefly discuss examples of application in plant, animal, and biomedical science. Taken as a whole, there are two main techniques used for CSIA, based on gas chromatography (GC) or liquid chromatography (LC) coupled to isotope ratio mass spectrometry (IRMS). The fact that CSIA requires instrument coupling (chromatography and IRMS) is an important aspect that constraints the interface between GC/LC and IRMS (usually, combustion or pyrolysis furnace (denoted as "C") with the GC; chemical oxidizer (denoted as "co"); or high-temperature combustion (referred to as "HTC") with the LC) and the type of metabolite that can be analyzed (typically, volatile or not). There are other possible couplings, such as GC-ICP-MS (gas chromatography-inductively coupled plasma-mass spectrometry), that may allow the determination of isotope ratios with a multicollector MS, but this approach has not been implemented in biology and will not be discussed here.

There is now quite a few published works taking advantage of GC-C-IRMS or LC-co-IRMS in plant science (typical examples in Table 1) and in biomedicine (Table 2). Quite generally, it has been shown that it is possible to measure the compound-specific isotope composition of amino acids (and derivatives such as glutathione), sugars, organic acids, alkanes, sterols, and base (nucleic acid) derivatives. Most popular

Table 1 Summary of Compound-Specific Isotope Analyses Applied to Plant Tissues

Matrix	Metabolites	Detection Methods and Isotopes	Application	References
Arabidopsis	Glu, Gln	LC-co-IRMS ^{13}C, GC-C-IRMS ^{13}C and ^{15}N	KIE of glutamine synthesis using $^{14}N/^{15}N$ and solvent isotope effects	Mauve et al. (2016)
Leaves from french bean plants	Sugars: Suc, Fruc, β-Glc, o-Fru, α-Glc	GC-C-IRMS ^{13}C	Determination of kinetic $^{12}C/^{13}C$ isotope fractionation by invertase	Mauve et al. (2009)
Leaf water in C3 and C4 plants	Phytol and sterols	GC-Py-IRMS ^{2}H	Hydrogen isotopic differences between C3 and C4 land-plant lipids	Zhou et al. (2016)
Bell pepper	*n*-Alkanes	GC-Py-IRMS ^{2}H	Pepper classification according to geographical origin	de Rijke et al. (2016)
Leaf from *Pinus sylvestris*	Carbohydrates	GC-Py-IRMS ^{18}O	Development derivatization methods	Lehmann et al. (2017)
Wheat grain	Amino acids	GC-C-IRMS ^{13}C and ^{15}N	Verification of the fertilization history of wheat crops	Paolini et al. (2015)
C3 and C4 plant	Sucrose: furancarboxaldehyde (i.e., furfural); HMF	GC-C-IRMS ^{13}C	Isotopic signature of carbohydrate pyrolysis products from C3 and C4 plants: Py-CSIA of C3 and C4 plant sugars	González-Pérez et al. (2016)
Vanilla pods	Vanillin	GC-C-IRMS ^{13}C and ^{2}H	Authentication, traceability	Hansen et al. (2014)
Macroalga (Ulva sp.)	DNA, RNA	LC/IRMS ^{13}C	DNA and RNA biosynthesis	Moerdijk-Poortvliet, Stal, and Boschker (2014)

Needle extract	Soluble carbohydrate	GC-Py-IRMS δ(18)O	δ(18)O sucrose of needles reflects the climatically controlled evaporative (18)O enrichment of leaf water	Zech et al. (2013)
Leguminous plants	aa	GC-C-IRMS ^{13}C	Biosynthetic pathways in plants	Styring et al. (2014)
Tobacco leaf	The wax and sterol fraction	2D (GC-C-IRMS)and high-temperature conversion (GC-HTC-IRMS)	Study of biosynthesis and delivery mechanisms of naturally occurring compounds in tobacco	Dumont et al. (2013)
Plant	aa	GC-C-IRMS ^{13}C	Study amino acid fluxes in a plant–microbe symbiotic association	Molero et al. (2011)
Plant	aa	GC-C-IRMS ^{13}C	Study carbon partitioning and dark respiration in cereals subjected to water stress	Aranjuelo et al. (2009)
Plant	Organics	LC/IRMS ^{13}C	Analysis of organic acids in plants	Hettmann et al. (2008)

Table 2 Summary of Compound-Specific Isotope Analyses Applied to Human and Animal Tissues

Matrix	Metabolites	Detection Methods and Isotopes	Application	References
Human plasma and urine	Short-chain fatty acids: acetate, propionate, butyrate	GC-C-IRMS ^{13}C	Influence of the type of indigestible carbohydrate on plasma and urine short-chain fatty acid	Verbeke et al. (2010) and Ferchaud-Roucher et al. (2006)
Human venous and arterial blood from the umbilical cord	Glutathione	GC-C-IRMS ^{13}C	In vitro measurement of fractional synthesis rate of glutathione	Tea et al. (2007)
Cancer culture cells and biopsie tissues	Amino acids, organic acids	GC-C-IRMS ^{13}C and ^{15}N LC-C-IRMS ^{13}C	Isotopic signature in cancer metabolism	Tea et al. (2016)
Milk and hair from infant	aa in proteins	GC-C-IRMS ^{15}N	Amino nitrogen transfer from human milk to infant hair protein	Tea et al. (2013) and Romek et al. (2013)
Lamb muscle	aa	GC-C-IRMS ^{15}N	Authentication and assessment of feed efficiency in ruminants	Cantalapiedra-Hijar et al. (2016)
Fat from pigs	FAME	GC-C-IRMS ^{13}C	Tool to ascertain the diet of Iberian pigs used	Recio et al. (2013)
Human and faunal from archeological samples	aa	LC-IRMS ^{13}C	Palaeodietary reconstructions	Webb et al. (2015)
Hair protein		GC-C-IRMS ^{15}N and ^{13}C	Vegetarians and omnivores are reflected in their hair protein ^{13}C and ^{15}N abundance	Petzke, Boeing, Klaus, and Metges (2005)

Human and animal tissues	aa	GC-C-IRMS ^{15}N	Refining human palaeodietary reconstruction	Styring et al. (2015)
Urine	Testosterone	GC-C-IRMS ^{13}C	IRMS detection of testosterone	Wang et al. (2014)
Urine		GC-Pyr-IRMS ^{2}H	Detecting target compounds for sports drug testing	Thevis et al. (2013)
Rat plasma and liver	Metabolites	GC-C-IRMS ^{13}C for lipids and LC-IRMS ^{13}C for glucose	Difference in ^{13}C of plasma metabolites and liver tissue between diabetic and nondiabetic Zucker diabetic fatty rats	Godin et al. (2013)
Human plasma	Cholesterol	GC-Pyr-IRMS ^{2}H	Determination of cholesterol absorption in normocholesterolemic volunteers	Godin et al. (2004)
	Glucose, fatty acids	GC-C-IRMS ^{13}C	Exercise performed immediately after fructose ingestion enhances fructose oxidation and suppresses fructose storage	Egli et al. (2016)
Plasma	Galactose, glucose	LC-IRMS ^{13}C	Quantitation of plasma ^{13}C-galactose and ^{13}C-glucose during exercise by liquid chromatography/isotope ratio mass spectrometry	Morrison et al. (2011)
Fecal sample	16s RNA	Anion-exchange LC-IRMS ^{13}C	Use of stable isotopes to measure the metabolic activity of the human intestinal microbiota	Reichardt et al. (2011)

applications are associated with sterols (doping control), amino acids (animal nutrition monitoring or plant ^{15}N labeling), or sugars (assessment of wine or honey adulteration). Up to now, ^{13}C and ^{15}N analyses in biology and biomedicine are more common than ^{18}O and ^{2}H (despite significant use for the analysis of volatile flavors, sometimes with coupling to headspace trapping, since the 2000s), simply because the latter cannot be performed by LC-co-IRMS and the use of the pyrolysis interface in GC-C-IRMS for oxygen and hydrogen isotopes can be difficult. For example, it is only recently that the $^{18}O/^{16}O$ ratio in plant sugars has been analyzed (Lehmann et al., 2017). Also, up to now, other isotopes such as sulfur ($^{34}S/^{32}S$ ratio) cannot be analyzed with the current techniques and require GC-ICP-MS. Thus, this chapter will focus on ^{13}C- and ^{15}N-CSIA.

2. COMPOUND-SPECIFIC ^{13}C AND ^{15}N ANALYSIS: HISTORY AND OVERVIEW

2.1 Brief History

Originally, CSIA was performed using off-line methods. They consisted of converting purified organic molecules to simple gases (CO_2 and N_2 for ^{13}C and ^{15}N analysis) in sealed quartz or metal tubes in the presence of oxidizing or reducing agents (de Groot, 2009). Gases were separated (isolated cryogenically) and then introduced to the IRMS via a dual-inlet system (Fig. 1A). This approach required tedious preparation samples and relatively large sample sizes. The concept of linking a GC with an IRMS was established in the mid- to late 1970s by Sano, Yotsui, Abe, and Sasaki (1976) and Matthews and Hayes (1978). In the early 1990s, the commercial production of the GC-C-IRMS provided a real breakthrough in CSIA. However, until 2000, the implementation of CSIA was very modest in biology as compared to geosciences. An alternative off-line technique consisted

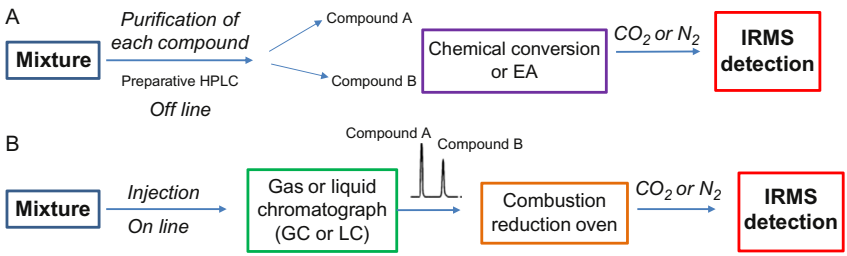

Fig. 1 Overview of instrumental coupling for CSIA, performed using off-line (A) and on-line methods (B).

of LC purification of compounds of interest using a preparative system (in which substantial amounts could be injected), and then isotope analysis by elemental analysis (EA) coupled to IRMS. This method has been used successfully for plant sugars and organic acids, for example (Duranceau, Ghashghaie, Badeck, Deleens, & Cornic, 1999). Then, LC-co-IRMS instruments were commercialized (in 2004) and enabled $^{13}C/^{12}C$ analysis. Recently, a system enabling both $^{13}C/^{12}C$ and $^{15}N/^{14}N$ analyses by LC coupled to IRMS via high-temperature combustion–desolvation (instead of chemical oxidation) has been proposed and is now available commercially (Federherr, Volders, Schmidt, Lange, & Sieper's, 2016). Both GC-C-IRMS and LC-co-IRMS on-line methods are relatively fast and allow the analysis of small quantities of sample (nmol of the compound of interest). Analytes are separated by GC or LC and converted quantitatively in gases in the interface, and finally transferred into the IRMS (principle summarized in Fig. 1B). These on-line techniques resulted in considerable increase in the number of studies using CSIA (Tables 1 and 2). However, it should be kept in mind that new developments remain relatively slow, because a critical step to carry out proper isotope analysis is sample preparation, from extraction to optimal derivatization and rigorous chromatographic conditions.

2.2 Overview of Sample Preparation and Analytical Strategies

In human and plant isotopic studies, advantage has been taken from other approaches such as metabolomics (including lipidomics) for standard sample extraction and preparation, and compound identification prior to isotope analysis. This is an important point: usual GC-C-IMRS or LC-co-IRMS instruments do not provide the identification of compounds separated by chromatography (IRMS only gives δ-values), and thus, biochemical identification should be performed beforehand, using GC-MS or LC-MS coupled to the same GC and LC conditions. Conversely, δ-values in individual metabolites provide information inaccessible with bulk stable isotope analyses (EA-IRMS) or mass spectrometers, and useful for metabolomics (e.g., to follow near natural abundance labeling). However, CSIA is more complex to undertake than bulk stable isotope analyses, simply because some isotope fractionation (see Box 1) may occur during the steps of sample preparation and/or chromatographic separation. Thus, to provide accurate δ-values in specific metabolites from biological tissues (i.e., leaves, roots, muscle) and fluids (plasma, urine, saliva), which both contain thousands of components (with highly variable chemical and physical properties),

BOX 1 Definitions

Analyte: compound analyzed by the instrument used that can be the metabolite itself (in LC systems) or a derivative of the metabolite of interest (in GC systems). A given metabolite can generate several analytes when the derivatization leads to several products. Conversely, a given analyte can originate from several metabolites, when the derivatization leads to identical products for distinct metabolites. For example, TMS-pyroglutamate is a shared analyte coming from both glutamine and glutamate upon silylation.

Derivatization: addition of chemical groups on metabolites of interest to improve their volatility (GC) or chromatographic separation (LC), or both.

δ-Value or isotope composition (usually expressed in ‰): abundance of the heavy isotope with respect to that of the light isotope, as compared to the international standard material. It is denoted as $\delta^{13}C$ for carbon and $\delta^{15}N$ for nitrogen.

Fractionation (Δ): isotopic difference (usually expressed in ‰) between the substrate and the product of a reaction. It is given by the deviation of the isotope effect (α) from 1, as $\Delta = \alpha - 1$. It can be shown that it can be calculated from δ-values in substrate and product as: $\Delta = (\delta_{substrate} - \delta_{product})/(\delta_{product} + 1)$.

Isotope effect (α): ratio of rate constants (k_{light}/k_{heavy}) or equilibrium constants (K_{light}/K_{heavy}) of the isotopologues of interest. For enzymatic reaction, it is the ratio of catalytic efficiency V/K: $\alpha = (V/K)_{light}/(V/K)_{heavy}$.

Isotopologue: isotopic analogue of a molecule, where one atom has been replaced by its isotope. For example, $^{13}C^{16}O_2$ is the ^{13}C-isotopologue of $^{12}C^{16}O_2$. Must not be confused with isotopomers, which refer to isotopic isomers (for example, $^{13}CH_3$–$^{12}CH_2OH$ and $^{12}CH_3$–$^{13}CH_2OH$ are two isotopomers of ethanol).

Isotope ratio mass spectrometer (IRMS): mass spectrometer based on a magnetic sector with (usually) fixed collectors (Faraday cups) adapted to quantify precisely the abundance of isotopic species of CO_2 (^{13}C analysis), N_2 (^{15}N analysis), CO (^{18}O analysis), H_2 (^{2}H analysis), or SO_2 (^{34}S analysis).

Quantitative reaction: chemical reaction that consumes all of the substrate molecules, thereby preventing any isotope fractionation. In nonquantitative reactions, substrate molecules left behind may have a δ-value different from the initial value because the reaction selects for an isotopic species (isotope effect).

it is crucial to pay attention to isotope behavior (i.e., possible isotope effects) at each step. These steps include: (i) extraction, (ii) derivatization (mostly, in GC-C-IRMS), and (iii) measurement itself. Fig. 2 shows an experimental workflow for the isolation of a great number of metabolites targeted for compound-specific stable isotope and structural analyses for plant, animal, and human applications. Before extraction, solid samples are preferably lyophilized and crushed (ground) to ensure homogeneity for bulk

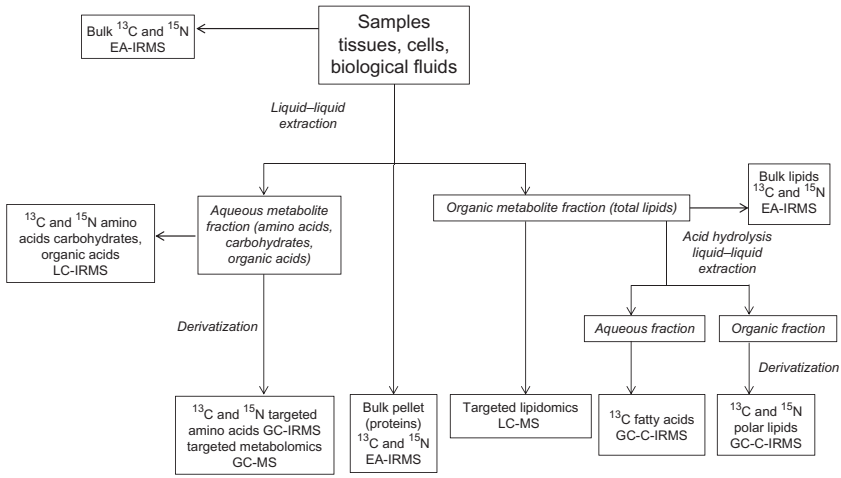

Fig. 2 Experimental workflow for the optimal isolation of a number of metabolites for CSIA for plant, animal, and human applications. This workflow integrates both bulk and compound-specific analyses as well as structural determination of metabolites so as to know the identity of compounds analyzed by GC-C-IRMS of LC-co-IRMS.

^{13}C and ^{15}N measurements and to increase the effectiveness of solvent penetration in the sample (extraction yield). The Bligh–Dyer method (Bligh & Dyer, 1959) is a well-known method originally used for lipids, and it can be used routinely for the liquid/liquid extraction of biological tissues. Two separated fractions are obtained: a total organic lipid fraction and an aqueous fraction (containing amino acids, carbohydrates, organic acids) to be analyzed by LC-co-IRMS and GC-MS, and then GC-C-IRMS after derivatization. The lipid fraction can be analyzed by LC-MS-targeted lipidomics, and bulk ^{13}C and ^{15}N abundance can be determined by EA-IRMS. The total lipid fraction includes polar lipids generally comprising fatty acids esterified to glycerol and polar headgroups (e.g., in phospholipids). Most commonly occurring polar lipids are phospholipids with choline or ethanolamine headgroups, i.e., phosphatidylcholine and phosphatidylethanolamine, while other polar lipids can include glycolipids (highly abundant in plant samples). Recently, CSIA of nitrogen-containing intact polar lipids by GC-C-IRMS has been published, for ^{15}N abundance in microbial phosphatidylethanolamine (Kayacelebi et al., 2015).

The step of functional group derivatization is inevitable in GC-C-IRMS just as in GC-MS. Indeed, metabolite classes found in biological samples are, for example, fatty acids, alcohol, monosaccharides, organic acids (carboxylic acids), and amino acids. Because of their functional groups (carboxylic,

hydroxyl, and amino groups) which are polar and nonvolatile, these metabolites are potentially undetectable by GC. Derivatization reactions like esterification, acetylation, and silylation are thus employed to improve chromatographic detection and separation. Meier-Augenstein (1997, 1999) and Rieley et al. (1994) provide an extensive review of derivatizing reagents common in GC-C-IRMS. It is worth mentioning that derivatizing reagents must conform to several criteria in order to avoid isotope fractionation: (i) quantitative reaction with analytes, (ii) limited addition of the element (N or C) being analyzed (i.e., to avoid isotope dilution and important corrections, see Box 2), (iii) no chromatographic isotope effects, and (iv) no detrimental effects on the reaction interface (furnace or chemical oxidizer). For ^{15}N and ^{13}C analysis it is thus essential to verify whether the analytical protocol introduces an isotope effect in every instance. In this context, the use of two types of internal standards is recommended: first, a molecule of a similar chemical structure (but not requiring derivatization) and of known isotope composition should be added to the sample prior to sample preparation. This standard allows one to check the reliability of the instrument and to correct for possible drifts of chromatographic isotope effects in δ-values. Second, a standard of a similar chemical structure requiring derivatization and of known isotope composition should be added to the sample prior to sample preparation. This standard allows one to check the stability of the isotopic correction and/or potential undesirable isotope effects affecting the observed δ-values. Moreover, due to the addition of carbon atoms (exogenous carbons of the derivatizing reagent), it is recommended to measure the δ-value of the second standard before and after derivatization, so as to calculate the isotope composition of the added carbon group by mass balance (see also Section 5).

3. COMPOUND-SPECIFIC ^{15}N ANALYSIS

Nitrogen stable isotope analysis by GC-C-IRMS has been mostly used for amino acids and was first implemented by Merritt and Hayes (1994). They used *N*-acetyl-*n*-propyl ester derivatives for GC separation. Later, *N*-pivaloyl isopropyl esters became preferred over acetyl derivatization (Metges, Petzke, & Hennig, 1996), because of the better chromatographic resolution. *N*-trifluoroacetyl anhydride (TFA) or *N*-pentafluoropropyl anhydride (PFPA) have been employed as alternative reagents in several studies (Docherty, Jones, & Evershed, 2001; Hofmann, Gehre, & Jung, 2003). It is important to note that ^{15}N-CSIA requires excellent GC conditions

BOX 2 Isotopic corrections after derivatization

Principle: chemical derivatization used in GC-C-IRMS leads to the addition of carbon atoms, while the IRMS gives the δ-value of CO_2 generated in the interface from the whole derivative. Therefore, the contribution of the exogenous C-atoms of the derivatizing reagent must be subtracted to calculate the true value of the metabolite. There are two main methods to get the isotope signature of derivatizing chemical groups:

- *Direct measurement*: the derivatizing reagent is analyzed by EA-IRMS (as a liquid sample), and thus, its δ-value is measured directly. Then, it is assumed that this value is fully representative of the added C-atoms in metabolite derivatives. This assumption may be incorrect if (i) the reagent contains C-atoms that do not belong to derivatizing groups (such as a solvent) or (ii) there is some isotope effects during derivatization.
- *Indirect measurement*: pure standard metabolites of known $\delta^{13}C$ are derivatized, and the isotope composition of added carbon is calculated from the observed δ-value of the derivative. This technique has the advantage to integrate all of the effects during preparation and separation, in a compound-specific manner. A series of standards of different δ-values can also be used (see later).

Calculation: the calculation of the actual $\delta^{13}C$ of the metabolite of interest is carried out by mass balance as follows:

$$\delta_{obs} = p \cdot \delta_{dev} + (1 - p) \cdot \delta_{act} \quad \text{(B1)}$$

where δ_{obs}, δ_{dev}, and δ_{act} are the $\delta^{13}C$ of the derivative (observed), the derivatizing groups, and of the metabolite of interest, respectively. p is the proportion of exogenous (added) carbon in the derivative. p is a critical parameter to be determined. Classical chemical rules can be used to predict the number of C-atoms added, using the known number of functional group effectively derivatized. However, such a prediction is often invalid with silylation because some methyl groups can be lost (e.g., $-Si(CH_3)_2$ groups instead of $-Si(CH_3)_3$) as well as carbon atoms from the metabolite itself (typically, whole $-COOSi(CH_3)_3$ groups) in the furnace of the GC-C-IRMS. This process is not easily predictable and depends on the metabolite of interest. It may thus be necessary to determine p using ^{13}C-enriched and ^{13}C-depleted standards so as to draw a calibration curve and determine p and δ_{dev} by linear regression, applying Eq. (B1).

Precision of δ-values: a caveat of derivatization with addition of C-atoms is that the isotopic correction increases the standard deviation (σ) on actual $\delta^{13}C$ values. In fact, Eq. (B1) can be rewritten as: $\sigma(\delta_{act}) = (\sigma(\delta_{obs}) + p \cdot \sigma(\delta_{dev}))/(1 - p)$. This means that the imprecision on measured δ-values is additive. Also, when the proportion of added carbon (p) is large, the denominator is small, and thus, $\sigma(\delta_{act})$ is large. For example, for trimethylsilylation of an amino acid-like glutamate with three functionalized groups, C-atom addition represents 65% of total carbon, and a typical σ of 0.2‰ on observed δ-values translates into a 1‰ uncertainty in δ_{act}.

and thus judicious selection of the GC column used in order to obtain good peak resolution and avoid coelution of analytes. Moreover, ^{15}N-CSIA involves combustion followed by reduction of nitrous oxides (NO_x) to N_2. The oxidation–reduction conversion is usually done using a combustion reactor with metallic catalysts (CuO/Pt, 850°C or CuO/NiO/Pt, 940°C), sometimes followed by a second reduction reactor (elemental Cu, at 600°C), thereby reducing nitrous oxides to N_2. Another important point to take into account for N-isotopic analyses is that gases (CO_2, N_2) are not separated downstream of the combustion interface, and therefore, CO_2 may enter the IRMS and yield significant ion current at m/z 28 and 29 due to CO^+ fragments. Consequently, it is essential to remove CO_2 from the carrier gas stream, and this is generally done by cryogenic trapping (−100°C).

3.1 *N*-pivaloylation of the Amine Functional Group

Derivatizaton as *N*-pivaloyl-*O*-isopropyl esters appears to be the best-adapted method for compound-specific ^{15}N analysis techniques (for, e.g., amino acids), since it does not involve addition of nitrogen-containing groups and does not produce by-products of metabolites of interest. Moreover, this derivatization reaction does not introduce heteroatoms like fluorine, which could lead to a nonquantitative sample conversion in the combustion furnace of the GC-C-IRMS. In fact, the presence of fluorinated in derivatives allows the formation of extremely stable forms of fluorides with Cu and/or Ni in the combustion furnace (such as CuF_2 and NiF_2), reducing the amount of available CuO and NiO and thus the efficacy of combustion catalysis. Other advantages of this method include good chromatographic quality and stability of derivatives (derivatized metabolites remain stable for several weeks, in contrast with methods like silylation where the derivatives may be degraded after only 1–2 days). Also, the pivaloyl group makes the compound more volatile and nonpolar as compared to acetyl groups, thereby improving chromatographic separation in most cases.

Nevertheless, not all amino acids can be analyzed using this method, either because they cannot be derivatized satisfactorily, or because they are imperfectly resolved in the chromatogram. A few years ago, a good resolution in the GC chromatogram was obtained with a mixture of 15 amino acids using a polar column (60 m ZB WAX, 100% polyethylene glycol) (Romek et al., 2013; Tea et al., 2013; Fig. 3). However, the resolution

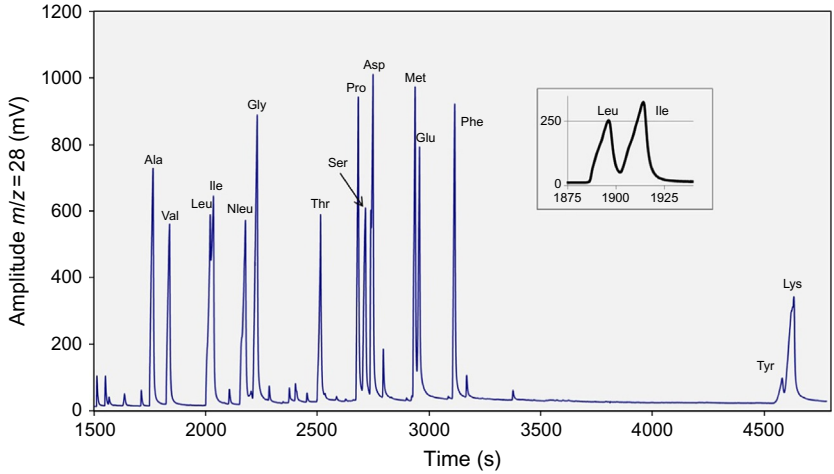

Fig. 3 Typical example of IRMS ^{15}N chromatogram (monitored by the signal from the collector of the major isotopic species at mass 28, $^{14}N_2$) showing the separation of 15 amino acids of a standard mixture in ethyl acetate (solvent), derivatized using the pivaloyl method. Each amino acid is present at 1.8 mg mL^{-1} (except for norleucine (internal standard) which is at 2 mg mL^{-1}). Inset shows the separation of Leu and Ile at 1 mg mL^{-1}.

of isomers of Leu and Ile and of the peaks of Tyr and Lys was not satisfactory. Amides like Asn or Gln, and Arg were not visible. Nevertheless, this derivatization had been effectively applied to the determination of $\delta^{15}N$ values in free amino acids (Petzke & Lemke, 2009), as well as amino acids from protein hydrolysates (Petzke & Lemke, 2009), hair samples (Petzke, Feist, Fleig, & Metges, 2006), and breast cancerous cells (Tea et al., 2016). Some amino acids such as arginine and glutamine, and polyamines like citrulline and ornithine are poorly detectable by this method, and thus, further work is needed to obtain their $\delta^{15}N$, possibly requiring an alternative derivatization approach.

3.2 *N,O*-trifluoroacetylation (TFA and PFPA)

Derivatizations to *N*-trifluoroacetyl isopropyl or *N*-pentafluoropropionyl esters are employed due to their excellent chromatographic properties compared with *N*-acetyl-isopropyl esters (NAIP). However, the compatibility with GC-C-IRMS is uncertain (i.e., δ-values are doubtful) due to the production of CuF_2 and NiF_2 in the combustion furnace of GC-C-IRMS (see earlier). In addition, it is necessary to reoxidize the combustion reactor every 30–40 runs to regenerate CuO, or even replace the furnace after 100–150

runs. The TFA method is suitable for most amino acids, but as for pivaloylation reaction, amides are poor reactants, leading to $\delta^{15}N$ values of Gln and Asn that represent mixed values from the acids and their amide counterparts. With classical methods, arginine is usually incompletely derivatized, since small amounts of ornithine and other by-products are formed. By contrast, the PFPA method allows one to fully derivatize arginine, as shown by classical GC-MS detection (Kayacelebi et al., 2015). Ornithine derivatization yields two products, in which the two primary amino groups are acylated differently, that is, one of the amino group gives a monosubstituted primary amide instead of a bisubstituted secondary amide. Our own preliminary results obtained by GC-C-IRMS show the presence of a unique peak of arginine derivative and two peaks for ornithine. However, $\delta^{15}N$ values including that of arginine were found to be strongly enriched (not shown here), simply reflecting the effect of fluorine, preventing a complete combustion reaction in the furnace and thus yielding CO that compromised $\delta^{15}N$ measurements. This analytical issue can be resolved by using a nonfluorinated analogue of PFPA derivatives, that is, NAIP.

Also, a polar chromatographic column can be used to improve resolution and avoid the problem of coelution observed with Lys, Cys, and Tyr, when using a non- or low-polar column. In fact, the choice of the GC column seems to be important to consider. It has been demonstrated that Chirasil-Val and DB-FFAP are unsuitable for such analyses, and that the HP-1MS column should be avoided to measure the $\delta^{15}N$ in amino acids (Chikaraishi, Takano, Ogawa, & Ohkouchi, 2010). This suggests that the stationary phase in these columns is too electrophilic, and therefore, the use of a DB-23, DB-35, HP-Chiral-20β, HPINNOWAX, and Ultra-2 columns should be preferred (Chikaraishi et al., 2010).

3.3 *tert*-Butyltrimethylsilylation

The *tert*-butyltrimethylsilylation (*t*-BDMS) reaction offers clear advantages in that the reaction is rapid and performed in one step only. The alkaline medium of the reaction assay also allows the simultaneous detection of glutamate and aspartate as well as their amide counterparts glutamine and asparagine. Beyond the ^{15}N analysis of amino acids, of particular interest in biomedical applications are other metabolites such as glutathione or taurine (a derivative of the sulfur-containing amino acid cysteine), which are involved in oxidative stress. The $\delta^{15}N$ in taurine has already been

measured by GC-C-IRMS (Tea, Antheaume, Besnard, & Robins, 2010), whereby the amino ($-NH_2$) and sulfonic acid ($-SO_3H$) groups are derivatized using triethylorthoacetate, without any $^{14}N/^{15}N$ isotope effect. Triethylorthoacetylation thus appears as an interesting alternative to silylation. In fact, a $^{14}N/^{15}N$ isotope effect would have been observed with "classical" trimethylsilylation, because it would have given a mixture of trimethylsilylated and dimethylsilylated taurine and a number of other by-products (Meier-Augenstein, 1997). One obvious disadvantage of this derivatization is the instability of derivatized products. Furthermore, glutamate, glutamine, and arginine undergo an incomplete reaction and/or generate by-products. Note that this situation is even worse with trimethylsilylation where arginine is broken down in ornithine, citrulline, and other products, and glutamine is partially deamidated to glutamate and pyroglutamate.

4. COMPOUND-SPECIFIC ^{13}C ANALYSIS

4.1 Principle and Precautions

As for ^{15}N analysis, the conversion of metabolites (or their derivatives) to the simple gas analyzed by IRMS (here, CO_2) must be quantitative. Combustion also produces H_2O as a major by-product, as well as NO_x and SO_x, in the case of metabolite containing N and S. NO_x and SO_x are corrosive, and furthermore, NO_2 interferes with CO_2 analysis (the m/z of $^{14}N^{16}O_2$ is 46, identical to $^{12}C^{16}O^{18}O$). These species are easily eliminated by a reactor that includes a reduction section (Cu at 500–700°C). Water can also participate in proton-transfer reactions within the IRMS ion source, leading to the formation of $^{12}C^{16}O_2H^+$ which interferes with $^{13}C^{16}O_2$ at m/z 45 (Leckrone & Hayes, 1998). Water is removed via a counter-current drier gas passed onto a selectively permeable membrane of sulfonated fluoropolymer (Nafion®). A cryogenic trap at −70°C that is placed downstream of GC can also be used to eliminate water. In most cases where GC-C-IRMS is used for derivatized compounds (e.g., sugars, amino acids), derivatization methods introduce exogenous carbon atoms, which alter the $\delta^{13}C$ values (the number of added carbon atoms can be quite high, for example, in the case of silylation). That is, the δ-value obtained with the IRMS is that of the analyte (derivatized metabolite) and thus does include the contribution of exogenous carbons, and this contribution should be removed by mass-balance calculations (Box 2).

4.2 Silylation

Silylation methods are the most commonly employed for the derivatization of metabolites (sterols, alcohols, amino acids, monosaccharides). In the case of polyfunctionalized compounds such as amino acids and monosaccharides, the number of carbons added by the derivatization is proportionally larger than in, e.g., sterols, due to their molecular weight. In principle, the silylation reaction is rapid and quantitative, and this is not accompanied by KIEs (Rieley et al., 1994). Prevalent methods for derivatization of amino acids and monosaccharides use *t*-BDMS or trimethylsilyl (TMS) derivatives. Unfortunately, they can lead to the formation of several products from one compound (i.e., mono-, di-, and tri-TMS and isomeric derivatives), and some compounds are degraded during the reaction (Meier-Augenstein, 1997; and see Section 3.3). It has been also demonstrated that silicon in *t*-BDMS and TMS groups may form silicon carbide (SiC_x) in the oxidation reactor of GC-C-IRMS, leading to incomplete analyte conversion to CO_2, thus causing an isotope fractionation (Shinebarger, Haisch, & Matthews, 2002). In addition, C-atoms trapping in Si forms are not easily quantifiable, and thus, it is difficult to determine the final proportion in exogenous carbon atoms; therefore, the isotopic correction to apply is highly uncertain. Furthermore, silicon derivatives such as SiC can undergo sublimation at high temperature (in the furnace) and then may enter the mass spectrometer and dirty the ion source. For these reasons, silylation is not the preferred method for ^{13}C analyses.

4.3 Acetylation/Methylboronation of Monosaccharides

An alternative approach to silylation and trifluoroacetylation methods (mentioned earlier for ^{15}N) is the use of acetylation by alkylchloroformates, which has widely been employed for functionalized hydroxyl groups of monosaccharides and amino or thiol groups of amino acids. Despite the KIE associated with the reaction, the method has been shown to be reproducible (i.e., the KIE is rather constant) and a correction can be implemented to calculate proper $\delta^{13}C$ values. A clear advantage is that derivatives are very stable compared to silylation (*t*-BDMS). S-containing metabolites such as cysteine and glutathione can be derivatized, and both glutamine and glutamate derivatives can be detected (Montigon, Boza, & Fay, 2001).

The technique of acetylation of monosaccharides forming alditol acetates has been adapted for GC-C-IRMS analysis, but typical analytical issues encountered in that case are: (i) a KIE during the reaction and (ii) a high

amount of added exogenous carbons in derivatives. To avoid the KIE associated with acetylation reactions, methylboronation (MBA) followed by trimethylsilylation can be employed. This approach leads to a lower carbon addition (+2 to 3 C-atoms per group) compared with alditol acetate derivatization (+10 to 12 C-atoms), but unfortunately, it has a low yield for several monosaccharides because it leads to an incomplete reaction with an associated KIE (van Dongen, Schouten, & Damsté, 2001).

4.4 Methylation of Fatty Acids and Methods Not Requiring Derivatization

Derivatization of fatty acids to fatty acid methyl esters (FAMEs) by the BF_3/methanol method is rapid and quantitative, thus avoiding isotopic fractionations. A correction is necessary to remove the contribution of the methyl C-atom introduced by the reagent. Instead, a simple procedure to avoid fatty acid methylation is the use of a DB-FFAP (nitroterephthalic acid-modified polyethyleneglycol) capillary GC column (typically 30 m, 0.32 mm i.d.). Fifteen fatty acids from C_{12} to C_{24} can be separated and analyzed by GC-C-IRMS with a total run time of 20 min. This method has already been validated in terms of specificity, linearity, precision, accuracy, sensitivity, and robustness, by using classical quantitative GC-FID (Zhang, Wang, & Liu, 2015), but has not been implemented for CSIA. However, this method is rapid and, importantly, does not add exogenous C-atoms.

4.5 LC-co-IRMS

The interface used to couple the LC system to the IRMS is now available commercially. It is based on the chemical wet oxidation, using sodium or ammonium peroxodisulfate (also simply referred to as "persulfate") and orthophosphoric acid as reactants to convert any metabolite containing carbon (organic molecule) to dissolved CO_2 within a reactor at 100°C. Then, the evolved CO_2 is extracted into a carrier gas by three gas-permeable membranes (one CO_2 separation unit and two water-extracting Nafion® membranes) and finally introduced into the IRMS (Fig. 4A). Recently, a new interface (Isochrom LC cube, manufactured by the company Elementar) has been commercialized and has the ability to perform both ^{13}C and ^{15}N analyses. In contrast to wet chemical oxidation used in previous systems, this new system uses a high-temperature combustion process with oxygen and platinum as a catalyst, oxidizing quantitatively metabolites into CO_2 and NO_x, subsequently reduced to N_2. It is thus referred to as

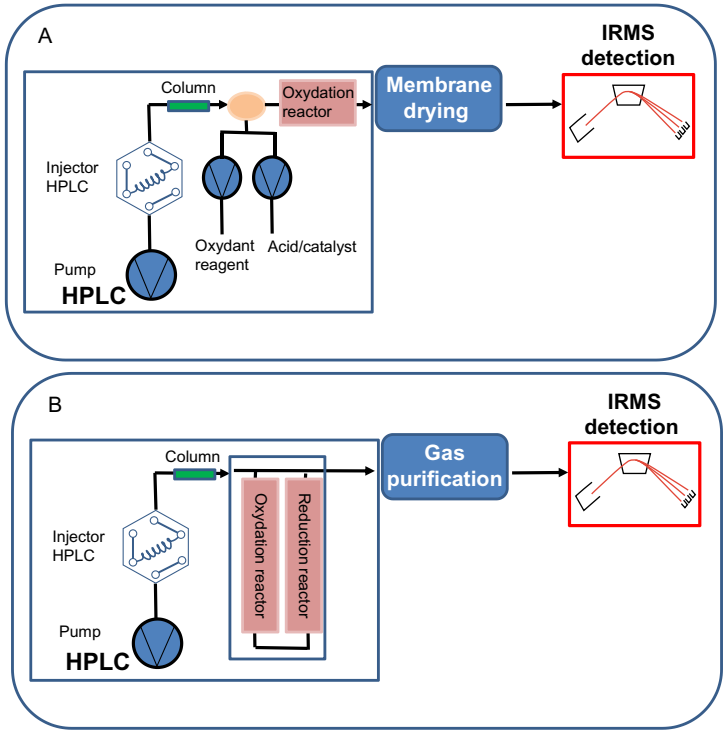

Fig. 4 Overview of the instrumental coupling in LC-C-IRMS systems, using (A) a flow reactor that mixes the aqueous sample with a strong oxidizing reagent and purges out carbon dioxide with a carrier gas or (B) the novel HTC interface technology based on catalyst-supported high-temperature combustion with subsequent gas purification/separation.

LC-HTC-IRMS. CO_2 and N_2 are purified by a selective trap or may be separated with a GC and then enter the IRMS (Fig. 4B). A proof of concept has been provided for the determination of both $\delta^{13}C$ and $\delta^{15}N$ in caffeine (Federherr et al., 2016).

LC-co- or LC-HTC-IRMS (collectively "LC-C-IRMS") is suitable for hydrosoluble molecules such as amino acids, nucleotides, sugars, peptides. The major advantage of LC-C-IRMS compared to GC-C-IRMS is that sample preparation does not require derivatization. Moreover, the isotopic precision of LC-C-IRMS is close to that of GC-C-IRMS. For example, the standard deviation of $\delta^{13}C$ values of underivatized amino acids in plasma was within 0.05‰–0.5‰, whereas the standard deviation of $\delta^{13}C$ values of the same amino acids derivatized and measured by GC-C-IRMS was within 0.2‰–0.6‰. However, there are critical analytical constraints associated

with LC-co-IRMS. First, the mobile phase in the LC can only be made of water or a saline aqueous solution so as not to adulterate δ-values with exogenous nitrogen or carbon. Second, chemical oxidation of N-containing compounds like urea can generate nitric or nitrous acid that can disproportionate to NO_2 (monoisotopic m/z 46), which can compromise $\delta^{13}C$ determination. Third, chemical oxidation is sensitive to chemical conditions such as the presence of metallic ions or chlorate that can be found in environmental (soil and plant) samples. Therefore, LC-co-IRMS will probably be rapidly replaced by LC-HTC-IRMS in the near future. Still, the general use of LC-C-IRMS requires perfect LC conditions and thus an adapted LC column, as well as temperature and eluent conditions.

5. KIE MEASUREMENT FROM LC-CO-IRMS OR GC-C-IRMS DATA

A KIE is defined by the relative rates of isotopologues (v and v^* for light and heavy isotopologues, respectively) during a reaction $A \rightarrow B$ that converts a substrate A (the concentration of which is denoted as (italicized) A and A^* for the light and heavy isotopologue, respectively) into a product B as follows:

$$\alpha = \frac{A^*/A}{v^*/v} \tag{1}$$

Since the reaction rate v can be written (by definition) as $v = -dA/dt$, this gives the following differential expression, by substitution into Eq. (1):

$$\alpha = \frac{d\ \ln(A)}{d\ \ln(A^*)} \tag{2}$$

In practice, the KIE is never measured applying Eq. (2) with reaction rates obtained with the natural (light) and isotopic (heavy) forms separately, because they are far too close to be distinguished from experimental noise (with the notable exception of hydrogen and deuterium). By contrast, the method that uses natural abundance is perfectly adapted because it allows very sensitive and precise monitoring of the isotope ratio in substrates and products of the reaction. Nevertheless, the isotope competition method (upon isotopic labeling) can be used despite a lower precision that the use of natural isotope ratios. The isotope competition method has been used recently for the determination of $^{16}O/^{18}O$ KIE in nucleotide cleavage, using

^{13}C monitoring of labeled substrates by LC-co-IRMS (Du, Ferguson, Gregory, & Sprang, 2008).

Depending on the mathematical expression of the reaction rate v and the reaction considered, the significance of α may change: for a first-order inorganic reaction, $v = kA$ (where k is the rate constant) and thus $\alpha = k/k^*$; for an enzyme that follows Michaelis–Menten kinetics, $\alpha = (V/K)/(V^*/K^*)$. In what follows, we give essential information on KIEs and how to exploit GC- and LC-co-IRMS data to calculate them. Further details on experimental procedures, general calculations, and applications to dissect enzyme mechanisms are given in Cleland (1980, 1995), O'Leary (1980), and Northrop (1981). As will be apparent below, the advantage of the GC- and LC-co-IRMS systems is that they allow substrate and product to be analyzed within one instrument, possibly simultaneously. This is particularly useful to determine the atomic site (atom position) at which the KIE applies. For example, in the reaction catalyzed by the glutamine synthetase, which converts glutamate $+NH_3$ into glutamine, the $^{14}N/^{15}N$ isotope effects at the α-amino and δ-amino sites were differentiated by the simultaneous analysis of glutamate and glutamine by GC-C-IRMS (Mauve et al., 2016). Also, when several substrates (or products) can be consumed (or evolved, respectively) by a biochemical process, they can be monitored simultaneously by LC- or GC-C-IRMS and individual KIEs can be measured. For example, KIEs in biotransformation of short hydrocarbons in mixtures have been examined by GC-C-IRMS (Kinnaman, Valentine, & Tyler, 2007), and KIEs in the oxidation products of nitrobenzene (nitrobenzyl alcohol and catechol) by dioxygenase have been monitored by LC-co-IRMS (Pati, Kohler, Bolotin, Parales, & Hofstetter, 2014). It is worth noting that the principles given below also apply for EIEs (reversible reactions). In such a case, the isotope composition is substrate and products must be measured at equilibrium. For a recent example using GC-C-IRMS, see Skarpeli-Liati et al. (2011).

5.1 Principle

Isotopic data on substrates and products of a biochemical reaction obtained from LC- or GC-C-IRMS instruments can be used to calculate the KIE. The general procedure that applies is similar to that already described extensively including for carboxylation or decarboxylation reactions (where the $\delta^{13}C$ in evolved CO_2 is monitored) (O'Leary, 1980). Quite generally, it exploits the relationship describing the Rayleigh fractionation, in which the isotope composition in the substrate of the reaction of interest at time

t (R_A) is expressed as a function of the initial isotope composition of the substrate (R_0) at $t=0$ and the commitment of the reaction (percentage of substrate consumed or product formed):

$$\ln(R_A) = \ln(R_0) + \left(\frac{1}{\alpha} - 1\right) \ln(\xi) \tag{3}$$

where ξ is the ratio of the concentration of the substrate remaining at time t to that present initially ($=A/A_0$). Eq. (3) remains valid regardless of the expression of the reaction rate (i.e., whether it is a single-step reaction or an enzymatic reaction). Note that Eq. (3) reflects the fact that when a reaction fractionates against the heavy isotope ($\alpha > 1$), the substrate should progressively be enriched (increase in R_A), reflecting the production of depleted products by mass balance (Fig. 5A). Also note that the isotope effect α is a constant and thus does not change with time t or commitment ξ. What changes with time is the isotope composition of the substrate and thus the isotopic difference between total product and substrate pools. By contrast, the instantaneous isotope ratio of the product formed at time t (that is, in differential terms, between t and $t+dt$), R_{Bt}, relates to that of remaining substrate at time t as follows: $R_{Bt} = v/v^* = R_A/\alpha$. Note that Eq. (3) can be rearranged to:

$$\alpha = \frac{\ln(\xi)}{\ln(\xi) + \ln\left(\frac{R_A}{R_0}\right)} \tag{4}$$

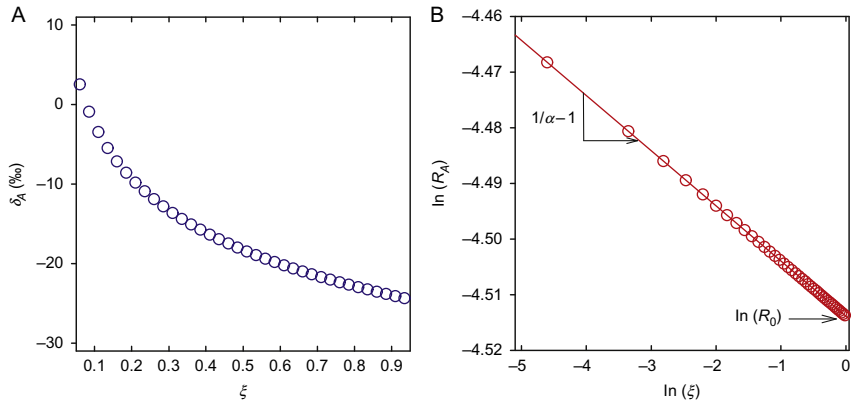

Fig. 5 Example of changes in δ-value of the substrate (δ_A) along a chemical reaction (A) and associated log–log plot (natural logarithm) to compute the KIE (B) using Eq. (3). The initial δ-value of the substrate (δ_0) was arbitrarily fixed at −25‰; note that the reaction proceeds from the *right* ($\xi=1$) to the *left* ($\xi=0$).

In practice, samples obtained from quenched reaction assays at different times (different values of ξ) are collected and the isotope composition in the substrate is measured. Then, the logarithm of the isotope ratio $\ln(R_A)$ is plotted against $\ln(\xi)$ and the slope gives $1/\alpha - 1$, using Eq. (3) (Fig. 5B). Alternatively, α can be calculated at each time point using Eq. (4).

At this stage, it is worth mentioning that the term "substrate" means the molecular species effectively consumed by the enzyme (or more generally, by the reaction). For example, the molecular species that binds to the enzyme can be involved in an equilibrium between different forms (e.g., between nonprotonated $-NH_2$ and protonated $-NH_3^+$), associated with an EIE (in this case, $^{15}\alpha_{eq}$ is about 1.015). This isotope effect has to be accounted for in calculations. An extensive description of equations associated with such calculations for ^{15}N has been provided in Mauve et al. (2016). Under certain circumstances, it is easier to carry out the isotopic analysis of the product (here denoted as B) rather than the substrate, because the substrate cannot be derivatized or chromatographically separated with available columns. This is typically the case for small compounds like NH_3 (NH_4^+) or HCO_3^- that are not separable with most columns routinely used for organic metabolites. The isotope composition of the product at time t is:

$$\ln(R_B) = \ln(R_0) + \ln\left(\frac{1-\xi^{1/\alpha}}{1-\xi}\right) \tag{5}$$

Eq. (5) can be rearranged to yield a linear relationship with $\ln(\xi)$ as follows:

$$\ln(R_0 - R_B(1-\xi)) = \ln(R_0) + \frac{1}{\alpha}\ln(\xi) \tag{6}$$

which can be reformulated using the relative amount of formed product ($= B/A_0 = 1 - A/A_0 = 1 - \xi$), denoted as g:

$$\ln(R_0 - R_B g) = \ln(R_0) + \frac{1}{\alpha}\ln(1-g) \tag{6'}$$

The isotope effect is thus given by:

$$\alpha = \frac{\ln(1-g)}{\ln\left(1 - \frac{R_B}{R_0}g\right)} \tag{7}$$

As with the substrate, the isotope effect can be computed using the slope of the relationship between $\ln(R_0 - R_B(1-\xi))$ and $\ln(\xi)$ with Eq. (6) or a direct calculation with Eq. (7).

5.2 Utilization of LC-co-IRMS and GC-C-IRMS Data

LC-co-IRMS and GC-C-IRMS data provide the isotope composition in analytes of interest (substrate or product of a reaction or their derivatives obtained during sample preparation, see Section 2). Typically for $^{13}C/^{12}C$ isotopes, exogenous carbon atoms might have been added by chemical derivatization to allow analysis by GC-C-IRMS, and this has first to be corrected for before using δ-values to compute isotope effects (Box 2). Importantly, values obtained by LC-co-IRMS and GC-C-IRMS represent average isotope values over the whole molecule. In other words, these techniques do not, usually, provide positional isotope compositions (exceptions being differentiation using substrate and products as in the glutamine synthetase reaction, or the use of molecular fragmentation prior to analysis). By contrast, KIEs are position specific. Primary KIE is associated with atom positions directly involved in the reaction coordinate (i.e., in bonds being made or broken). Secondary KIEs arise due to changes in bonding at other atoms in the molecule. Thus, the isotope effect that is computed from LC-co-IRMS and GC-C-IRMS data is the average across positions. For example, if a molecule contains n carbon atoms and only one C-atom is involved in bonds being reshuffled during the reaction, the net observed $^{12}C/^{13}C$ isotope effect value will be:

$$\alpha = \frac{\alpha_{\text{int}} + (n-1)}{n} \tag{8}$$

where α_{int} is the intrinsic isotope effect at the C-atom position of interest. Of course, from a biochemical perspective, the relevant parameter is α_{int} because it gives information on the mechanism of catalysis. Eq. (8) assumes that there is no secondary isotope effect so that $(n-1)$ is not multiplied by anything in the numerator. This assumption is sometimes reasonable, because secondary isotope effects (i.e., on other, nondirectly involved atom positions) are generally small (i.e., close to 1.000). Eq. (8) also applies to other elements (N, H, O) when there are n atoms and a positional isotope effect α_{int}. It can even be the case for nitrogen, since some metabolites may have more than one N-atom (e.g., glutamine, arginine).

An important caveat of KIE measurements by these techniques is the precision that can be achieved. It is not unusual to observe standard deviations on standards or samples larger than 0.2‰, or even 0.5‰. By differentiating Eq. (4) at fixed ξ (i.e., at fixed time) and using the definition of the isotope composition ($\delta = R/R_{st} - 1$), we can easily obtain a relationship between the variation in the δ-value of the substrate, $\Delta\delta_A$, and the resulting change in the observed KIE, $\Delta\alpha$:

$$\Delta\alpha = -\frac{\Delta\delta_A}{\delta_A + 1} \cdot \frac{\ln(\xi)}{\left(\ln(\xi) + \ln\left(\frac{\delta_A + 1}{\delta_0 + 1}\right)\right)^2} \tag{9}$$

Eq. (9) shows that at the beginning of the reaction, $\ln(\xi)$ is small and the denominator of the right term does cause a large error in α. In other words, because we are at the beginning at the reaction, the actual change in δ_A as compared to δ_0 is rather small, and thus, a measurement error in δ_A, even modest, is proportionally very large compared to the difference $\delta_0 - \delta_A$. Conversely, near the end of the reaction, where $\ln(\xi)$ goes to very negative values, the right term tends to 1 and the error in α can be modest. This situation can nevertheless be problematic from an experimental point of view because under such circumstances, nearly all of the substrate is consumed, the concentration in A is small, and therefore measuring δ_A is potentially very difficult (meaning that $\Delta\delta_A$ can be large). This situation is reversed with the product (measurement of δ_B): at the beginning of the reaction, the product is present in small amounts and thus measuring its isotope composition can also be difficult. A numerical example of Eq. (9) is given in Fig. 6, where the actual isotope effect is fixed at $\alpha = 1.010$, the analytical error on δ_A is fixed at 0.2‰, and the initial substrate has an isotope composition (δ_0) of −25‰. At low reactional commitment ($\xi = 0.9$), the error made on observed α is about 2‰, while at high commitment ($\xi = 0.1$), the error is only 0.1‰. Again, in practice, $\Delta\delta_A$ is not constant and tends to increase at low concentration. It is therefore critical to ensure a good linearity of the IRMS and has isotopic standards (including internal standards) to have a reliable δ-value. It should be noted that a modest error in observed α of about 1‰ can be highly problematic because the resulting error in α_{int} is much larger (Eq. 8).

It is apparent in Eqs. (3)–(7) that the commitment of the reaction (measured as the fraction of remaining substrate (ξ) or the fraction of appeared

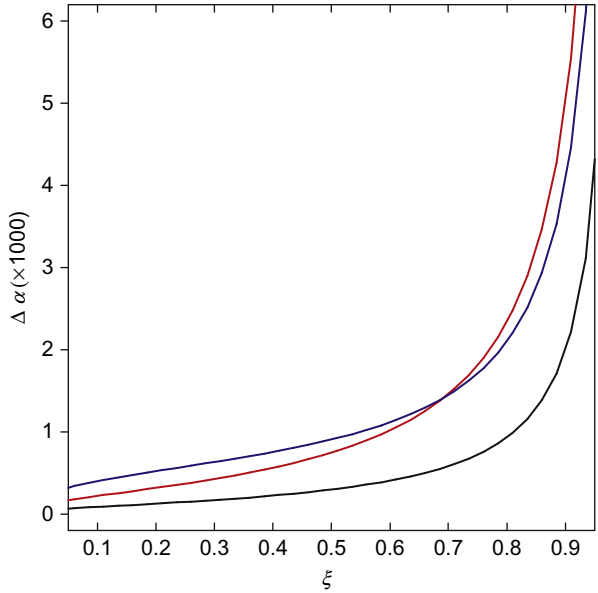

Fig. 6 Potential error in KIE determination ($\Delta\alpha$) as a function of the fraction of remaining substrate ξ when there is an uncertainty in measured δ-values of the substrate ($\Delta\delta$), as predicted by Eq. (9). *Black*, fixed $\Delta\delta$ of 0.2‰; *red*, fixed $\Delta\delta$ of 0.5‰; *blue*, varying $\Delta\delta$ (increasing from 0.35‰ to 1‰ as the reaction proceeds). In this example, the actual KIE of the reaction is 1.010; for example, at high ξ, $\Delta\alpha$ is 0.006 (6‰) or more, meaning that the observed value of the KIE ranges within 1.004 and 1.016.

product (g)) is an important parameter to be determined. GC-C-IRMS and LC-co-IRMS analyses may give the opportunity to measure precisely the amount of substrate and/or product when they are carried out in the split mode, i.e., when a fraction of the injected sample ends up to the LC or GC detector after the chromatography. Unfortunately, this method is compromised when the splitless mode is used to compensate for a low metabolite concentration and thus increase the signal in IRMS collectors. A compromise can be the use of a low split ratio (of, say, 5%) so that most of the injected sample ends up being analyzed by the IRMS. Alternatively, one may use the signal of the major mass (44 for carbon, 28 for nitrogen) to estimate the amount of material being analyzed (Tea et al., 2013). Of course, this requires a specific calibration curve to be done because the response of the collectors (in amperes or volts) is highly sensitive to analytical conditions such as the level of background signal.

5.3 Example

Here, we provide an example associated with the $^{12}C/^{13}C$ isotope effect in the catalysis of glycolate oxidase (GOX). This enzyme converts glycolate into glyoxylate, using O_2 as an oxidant and a flavine (FMN) as a cofactor. The KIE of the reaction has been determined recently by LC-co-IRMS, by following the $\delta^{13}C$ value of the substrate (glycolate) and the amount of remaining glycolate using refractometry (Dellero et al., 2015).

In that study, purified recombinant GOX was assayed in vitro and the reaction was quenched at different times using hydrochloric acid. Samples were lyophilized and resuspended in distilled water, and a volume of the resulting solution corresponding to 10–100 nmol of C in glycolate was injected into the LC-co-IRMS system. The LC allowed separation of the buffer (*tris*), glycolate, and glyoxylate by anion-exchange chromatography, with isocratic degassed water as the mobile phase. Detection was performed using a refractometer, and thus, glycolate amounts were determined with the LC signal (using a calibration curve). The split mode diverts one part of the sample to the LC detector, and the IRMS only sucks one fraction of the incoming sample (possibly via an interfacing needle valve), and therefore, the effective C amount entering the IRMS for isotopic analysis is much lower than 10 nmol (rather within the 100–1000 pmol range). The relationship obtained between reactional commitment and the logarithm of the isotope ratio is shown in Fig. 7, with the range of experimental values shown by gray shading. It is clear that at the beginning of the reaction, the potential error is relatively small, simply because the substrate is at high concentration (leading to a small analytical variability), and any variation of α (biological variability) does not translate into a big change in $\delta^{13}C$ of the substrate. However, as the reaction proceeds, both the lower concentration and the biological variability can lead to large uncertainty in the experimental points. This means that in the plot shown in Fig. 7B, the estimate of the intercept ($\ln(R_0)$) will be rather reliable (if not already known), while the slope (given by $1/\alpha - 1$, see Eq. 3) and thus the KIE may be associated with a large error. In that case, the average $^{12}C/^{13}C$ isotope effect is 1.019 and its standard deviation is 4‰, which is not negligible.

The $^{12}C/^{13}C$ isotope effect has also been determined using deuterated glycolate (Fig. 7, red curves). Under such circumstances, α-protonation of glycolate is slowed down and an increase in the $^{12}C/^{13}C$ isotope effect is expected. As a matter of fact, a value of 1.046 is found. When plotted together, it appears that the first time points (high $\ln(\xi)$ values) are close

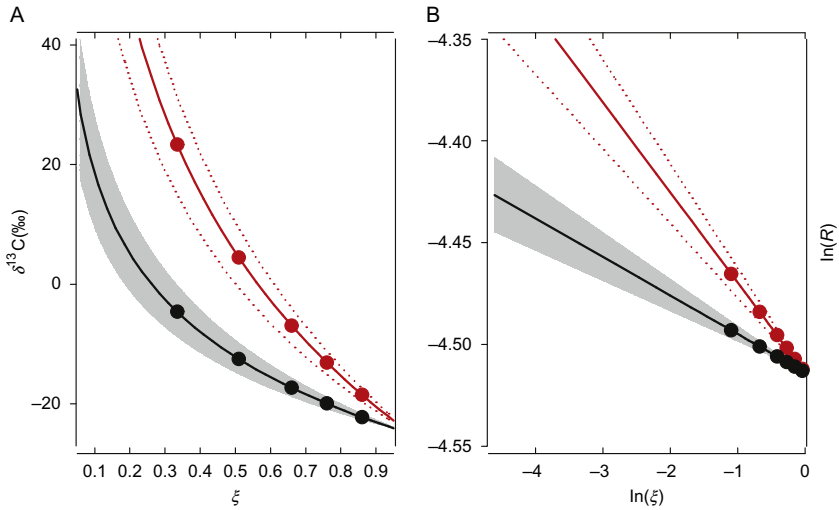

Fig. 7 Relationship between reaction commitment (fraction of remaining substrate, ξ) and the δ-value in substrate glycolate during the reaction catalyzed by *Arabidopsis* glycolate oxidase (A); and associated log–log relationship (natural logarithm) between ξ and the $^{13}C/^{12}C$ isotope ratio (B). *Black*, reaction with natural protonated glycolate; *red*, reaction with deuterated glycolate. *Solid lines*, *curves* driven by experimental points (means). *Dotted and shaded zones* represent regions of 80% confidence of measurement values (i.e., ± standard deviation). Note nearly indistinguishable data points on the *right hand side* of (B).

to those of the curve obtained with ordinary glycolate (Fig. 7B). This reflects the effect described by Eq. (9) whereby at low commitment, even very small variations in the δ-value of the substrate can cause large errors in observed α. That is, the relative change in δ_A (as compared to δ_0) is small and does not allow facile differentiation between distinct kinetic curves. In that respect, $\delta^{13}C$ values obtained at large commitment can be seen as essential, but unfortunately, they are associated with larger analytical errors.

Taken as a whole, accuracy and precision of GC-C-IRMS and LC-co-IRMS data are especially important to ensure good KIE determination. To do so, both replicating samples (assays) and running analyses within the same concentration range (e.g., using sample pooling for aliquots collected at low ξ) to avoid linearity bias (see Hartenbach et al., 2008 for an example of atrazine analysis by GC-C-IRMS) represent good practice to minimize potential errors in α.

6. CONCLUSIONS AND PERSPECTIVES

The potential of CSIA is enormous because of the variety of applications, from soil science to biomedicine. In fact, it is now well recognized that bulk isotope composition of tissues or organic matter is not a sufficient base to understand physiological mechanisms. For example, one of the most important applications of carbon isotopes worldwide is the use of $\delta^{13}C$ to select crop varieties with a better water use efficiency (Farquhar & Richards, 1984). Nonetheless, it is clear that this principle still needs refinements because of the multiplicity of isotope effects in metabolism and the nonhomogenous distribution of ^{13}C between plant metabolites (Tcherkez, Mahe, & Hodges, 2011). Presently, we believe that three lines of improvement warrant further work: First, CSIA extended to other elements such as oxygen and hydrogen (still in its infancy in biology and medicine) and sulfur (nearly nonexisting currently). Second, techniques other than GC-C-IRMS and LC-C-IRMS, such as high-resolution mass spectrometry (such as the Orbitrap® used in LC-MS that can potentially resolve ^{13}C and ^{15}N isotopologues, for example). Third, intramolecular isotope analysis is desirable, simply because the isotope composition within metabolites is heterogeneous due to position-specific isotope effects. In fact, considerable progress has been done on sugars using ^{13}C-NMR (for a review, see Gilbert, Silvestre, Robins, Remaud, & Tcherkez, 2012), but also GC-pyrolysis-IRMS in small organic acids (e.g., Dias, Freeman, & Franks, 2002).

ACKNOWLEDGMENTS

The authors thank the support of the initiative PLAISIR (Pays de la Loire Association for International Structure on "Isotopomic Research") funded by the French Regional International Strategy Grant Pays de la Loire, and the Australian Research Council through a Future Fellowship grant (under contract FT140100645).

REFERENCES

Aranjuelo, I., Cabrera-Bosquet, L., Mottaleb, S. A., Araus, J. L., & Nogués, S. (2009). $^{13}C/^{12}C$ isotope labeling to study carbon partitioning and dark respiration in cereals subjected to water stress. *Rapid Communications in Mass Spectrometry*, *23*, 2819–2828.

Bligh, E., & Dyer, J. (1959). A rapid method of total lipid extraction and purification. *Canadian Journal of Biochemistry and Physiology*, *37*, 911–917.

Cantalapiedra-Hijar, G., Ortigues-Marty, I., Schiphorst, A.-M., Robins, R. J., Tea, I., & Prache, S. (2016). Natural ^{15}N abundance in key amino acids from lamb muscle: Exploring a new horizon in diet authentication and assessment of feed efficiency in ruminants. *Journal of Agricultural and Food Chemistry*, *64*, 4058–4067. acs.jafc.6b00967.

Chikaraishi, Y., Takano, Y., Ogawa, N. O., & Ohkouchi, N. (2010). Instrumental optimization of compound-specific nitrogen isotope analysis of amino acids by gas chromatography/combustion/isotope ratio mass spectrometry. In N. Ohkouchi, I. Tayasu, & K. Koba (Eds.), *Earth, life, and isotopes*. Kyoto: Kyoto University Press, pp. 367–386.

Cleland, W. W. (1980). Measurement of isotope effects by the equilibrium perturbation technique. *Methods in Enzymology*, *64*, 104–125.

Cleland, W. W. (1995). Isotope effects: Determination of enzyme transition state structure. *Methods in Enzymology*, *249*, 341–373.

de Groot, P. A. (2009). *Handbook of stable isotope analytical techniques. Vol. 2*. Ham, Belgium: Elsevier.

Dellero, Y., Mauve, C., Boex-Fontvieille, E., Flesch, V., Jossier, M., Tcherkez, G., et al. (2015). Experimental evidence for a hydride transfer mechanism in plant glycolate oxidase catalysis. *The Journal of Biological Chemistry*, *290*, 1689–1698.

de Rijke, E., Truyols, V., & de Koster, C. G. (2016). UvA-DARE (digital academic repository) the use of ^{2}H and ^{18}O isotopic analyses combined with chemometrics as a traceability tool for the geographical origin of bell peppers. *Food Chemistry*, *204*, 122–128.

Dias, R. F., Freeman, K. H., & Franks, S. G. (2002). Gas chromatography–pyrolysis–isotope ratio mass spectrometry: A new method for investigating intramolecular isotopic variation in low molecular weight organic acids. *Organic Geochemistry*, *33*, 161–168.

Docherty, G., Jones, V., & Evershed, R. P. (2001). Practical and theoretical considerations in the gas chromatography/combustion/isotope ratio mass spectrometry $\delta^{13}C$ analysis of small polyfunctional compounds. *Rapid Communications in Mass Spectrometry*, *15*, 730–738.

Du, X., Ferguson, K., Gregory, R., & Sprang, S. R. (2008). A method to determine ^{18}O kinetic isotope effects in the hydrolysis of nucleotide triphosphates. *Analytical Biochemistry*, *372*, 213–221.

Dumont, E., Tienpont, B., Higashi, N., Mitsui, K., Ochiai, N., Kanda, H., et al. (2013). Heart-cutting two-dimensional gas chromatography in combination with isotope ratio mass spectrometry for the characterization of the wax fraction in plant material. *Journal of Chromatography A*, *1317*, 230–238.

Duranceau, M., Ghashghaie, J., Badeck, F., Deleens, E., & Cornic, G. (1999). $\delta^{13}C$ of CO_2 respired in the dark in relation to $\delta^{13}C$ of leaf carbohydrates in Phaseolus vulgaris L. under progressive drought. *Plant, Cell & Environment*, *22*, 515–523.

Egli, L., Lecoultre, V., Cros, J., Rosset, R., Marques, A.-S., Schneiter, P., et al. (2016). Exercise performed immediately after fructose ingestion enhances fructose oxidation and suppresses fructose storage. *American Journal of Clinical Nutrition*, *103*, 348–355.

Elsner, M., & Imfeld, G. (2016). Compound-specific isotope analysis (CSIA) of micropollutants in the environment—Current developments and future challenges. *Current Opinion in Biotechnology*, *41*, 60–72.

Farquhar, G., & Richards, R. (1984). Isotopic composition of plant carbon correlates with water-use efficiency of wheat genotypes. *Australian Journal of Plant Physiology*, *11*, 539.

Federherr, E., Volders, F., Schmidt, C., & Lange, L. (2016). A novel LC-IRMS interface for flexible compound-specific stable isotope analysis. *Rapid Communications in Mass Spectrometry*, *30*, 944–952.

Ferchaud-Roucher, V., Albert, C., Champ, M., & Krempf, M. (2006). Solid-phase microextraction method for carbon isotopic analysis of volatile carboxylic acids in human plasma by gas chromatography/combustion/isotope ratio mass spectrometry. *Rapid Communications in Mass Spectrometry*, *20*, 3573–3578.

Gilbert, A., Silvestre, V., Robins, R. J., Remaud, G. S., & Tcherkez, G. (2012). Biochemical and physiological determinants of intramolecular isotope patterns in sucrose from C_3, C_4 and CAM plants accessed by isotopic ^{13}C NMR spectrometry: A viewpoint. *Natural Product Reports*, *29*, 476.

Godin, J.-P., Richelle, M., Metairon, S., & Fay, L.-B. (2004). [2H/H] isotope ratio analyses of [2H5]cholesterol using high-temperature conversion elemental analyser isotope-ratio mass spectrometry: Determination of cholesterol absorption in normocholesterolemic volunteers. *Rapid Communications in Mass Spectrometry*, *18*, 325–330.

Godin, J.-P., Ross, A. B., Cléroux, M., Pouteau, E., Montoliu, I., Moser, M., et al. (2013). Natural carbon isotope abundance of plasma metabolites and liver tissue differs between diabetic and non-diabetic Zucker diabetic fatty rats. C. Miele, Ed. *PLoS One*, *8*. e74866.

González-Pérez, J. A., Jiménez-Morillo, N. T., de la Rosa, J. M., Almendros, G., & González-Vila, F. J. (2016). Compound-specific stable carbon isotopic signature of carbohydrate pyrolysis products from C3 and C4 plants. *Journal of the Science of Food and Agriculture*, *96*, 948–953.

Hansen, A. M. S., Fromberg, A., & Frandsen, H. (2014). Authenticity and traceability of vanilla flavors by analysis of stable isotopes of carbon and hydrogen. *Journal of Agricultural and Food Chemistry*, *62*(42), 10326–10331.

Hartenbach, A. E., Hofstetter, T. B., Tentscher, P. R., Canonica, S., Berg, M., & Schwarzenbach, R. P. (2008). Carbon, hydrogen, and nitrogen isotope fractionation during light-induced transformations of atrazine. *Environmental Science and Technology*, *42*, 7751–7756.

Hettmann, E., Gleixner, G., & Juchelka, D. (2008). *irm-LC/MS: $\delta^{13}C$ analysis of organic acids in plants*. Thermo Scientific (Application note 30075).

Hofmann, D., Gehre, M., & Jung, K. (2003). Sample preparation techniques for the determination of natural $^{15}N/^{14}N$ variations in amino acids by gas chromatography-combustion-isotope ratio mass spectrometry (GC-C-IRMS). *Isotopes in Environmental and Health Studies*, *39*, 233–244.

Kayacelebi, A. A., Knöfel, A.-K., Beckmann, B., Hanff, E., Warnecke, G., & Tsikas, D. (2015). Measurement of unlabeled and stable isotope-labeled homoarginine, arginine and their metabolites in biological samples by GC–MS and GC–MS/MS. *Amino Acids*, *47*, 2023–2034.

Kinnaman, F. S., Valentine, D. L., & Tyler, S. C. (2007). Carbon and hydrogen isotope fractionation associated with the aerobic microbial oxidation of methane, ethane, propane and butane. *Geochimica et Cosmochimica Acta*, *71*, 271–283.

Leckrone, K. J., & Hayes, J. M. (1998). Water-induced errors in continuous-flow carbon isotope ratio mass spectrometry. *Analytical Chemistry*, *70*, 2737–2744.

Lehmann, M. M., Gamarra, B., Kahmen, A., Siegwolf, R. T. W., & Saurer, M. (2017). Oxygen isotope fractionations across individual leaf carbohydrates in grass and tree species. *Plant, Cell & Environment*, *40*, 1658–1670.

Matthews, D. E., & Hayes, J. M. (1978). Isotope-ratio-monitoring gas chromatography-mass spectrometry. *Analytical Chemistry*, *50*, 1465–1473.

Mauve, C., Bleton, J., Bathellier, C., Lelarge-Trouverie, C., Guerard, F., Ghashghaie, J., et al. (2009). Kinetic $^{12}C/^{13}C$ isotope fractionation by invertase: Evidence for a small *in vitro* isotope effect and comparison of two techniques for the isotopic analysis of carbohydrates. *Rapid Communications in Mass Spectrometry*, *23*, 2499–2506.

Mauve, C., Giraud, N., Boex-Fontvieille, E. R. A., Antheaume, I., Tea, I., & Tcherkez, G. (2016). Kinetic commitment in the catalysis of glutamine synthesis by GS1 from Arabidopsis using $^{14}N/^{15}N$ and solvent isotope effects. *Plant Physiology and Biochemistry*, *108*, 203–211.

Meier-Augenstein, W. (1997). The chromatographic side of isotope ratio mass spectrometry: Pitfalls and answers. *LCGC International*, *15*, 244–253.

Meier-Augenstein, W. (1999). Applied gas chromatography coupled to isotope ratio mass spectrometry. *Journal of Chromatography A*, *842*, 351–371.

Merritt, D. A., & Hayes, J. M. (1994). Nitrogen isotopic analyses by isotope-ratio-monitoring gas chromatography/mass spectrometry. *Journal of the American Society for Mass Spectrometry*, *5*, 387–397.

Metges, C. C., Petzke, K.-J., & Hennig, U. (1996). Gas chromatography/combustion/isotope ratio mass spectrometric comparison of N-acetyl- and N-pivaloyl amino acid esters to measure 15N isotopic abundances in physiological samples: A pilot study on amino acid synthesis in the upper gastro-intestinal tract of minipigs. *Journal of Mass Spectrometry*, *31*, 367–376.

Moerdijk-Poortvliet, T. C. W., Stal, L. J., & Boschker, H. T. S. (2014). LC/IRMS analysis: A powerful technique to trace carbon flow in microphytobenthic communities in intertidal sediments. *Journal of Sea Research*, *92*, 19–25.

Molero, G., Aranjuelo, I., Teixidor, P., Araus, J. L., & Nogués, S. (2011). Measurement of 13C and 15N isotope labeling by gas chromatography/combustion/isotope ratio mass spectrometry to study amino acid fluxes in a plant-microbe symbiotic association. *Rapid Communications in Mass Spectrometry*, *25*, 599–607.

Montigon, F., Boza, J. J., & Fay, L. B. (2001). Determination of13C- and15N-enrichment of glutamine by gas chromatography/mass spectrometry and gas chromatography/combustion/isotope ratio mass spectrometry after N(O,S)-ethoxycarbonyl ethyl ester derivatisation. *Rapid Communications in Mass Spectrometry*, *15*, 116–123.

Morrison, D. J., O'Hara, J. P., King, R. F. G. J., & Preston, T. (2011). Quantitation of plasma 13C-galactose and 13C-glucose during exercise by liquid chromatography/isotope ratio mass spectrometry. *Rapid Communications in Mass Spectrometry*, *25*, 2484–2488.

Northrop, D. B. (1981). The expression of isotope effects on enzyme-catalyzed reactions. *Annual Review of Biochemistry*, *50*, 103–131.

O'Leary, M. H. (1980). Determination of heavy-atom isotope effects on enzyme-catalyzed reactions. *Methods in Enzymology*, *64*, 83–104.

Paolini, M., Ziller, L., Laursen, K. H., Husted, S., & Camin, F. (2015). Compound-specific $\delta^{15}N$ $\delta^{13}C$ analyses of amino acids for potential discrimination between organically and conventionally grown wheat. *Journal of Agricultural and Food Chemistry*, *63*, 5841–5850.

Pati, S. G., Kohler, H.-P. E., Bolotin, J., Parales, R. E., & Hofstetter, T. B. (2014). Isotope effects of enzymatic dioxygenation of nitrobenzene and 2-nitrotoluene by nitrobenzene dioxygenase. *Environmental Science and Technology*, *48*, 10750–10759.

Petzke, K. J., Boeing, H., Klaus, S., & Metges, C. C. (2005). Carbon and nitrogen stable isotopic composition of hair protein and amino acids can be used as biomarkers for animal-derived dietary protein intake in humans. *Journal of Nutrition*, *135*(6), 1515–1520.

Petzke, K. J., Boeing, H., & Metges, C. C. (2005). Choice of dietary protein of vegetarians and omnivores is reflected in their hair protein13C and15N abundance. *Rapid Communications in Mass Spectrometry*, *19*, 1392–1400.

Petzke, K. J., Feist, T., Fleig, W. E., & Metges, C. C. (2006). Nitrogen isotopic composition in hair protein is different in liver cirrhotic patients. *Rapid Communications in Mass Spectrometry*, *20*, 2973–2978.

Petzke, K. J., & Lemke, S. (2009). Hair protein and amino acid ^{13}C and ^{15}N abundances take more than 4 weeks to clearly prove influences of animal protein intake in young women with a habitual daily protein consumption of more than 1 g per kg body weight. *Rapid Communications in Mass Spectrometry*, *23*, 2411–2420.

Recio, C., Martín, Q., Raposo, C., & Raposo, C. (2013). GC-C-IRMS analysis of FAMEs as a tool to ascertain the diet of Iberian pigs used for the production of pork products with high added value. *Grasas y Aceites*, *64*, 181–190.

Reichardt, N., Barclay, A. R., Weaver, L. T., & Morrison, D. J. (2011). Use of stable isotopes to measure the metabolic activity of the human intestinal microbiota. *Applied and Environmental Microbiology*, *77*, 8009–8014.

Rieley, G., Brand, W., Mersch, F. J., Garritt, R., Fenwick, C. S., & Fallick, A. E. (1994). Derivatization of organic compounds prior to gas chromatographic–combustion–isotope ratio mass spectrometric analysis: Identification of isotope fractionation processes. *The Analyst*, *119*, 915–919.

Romek, K. M., Julien, M., Frasquet-Darrieux, M., Tea, I., Antheaume, I., Hankard, R., et al. (2013). Human baby hair amino acid natural abundance ^{15}N-isotope values are not related to the ^{15}N-isotope values of amino acids in mother's breast milk protein. *Amino Acids*, *45*, 1365–1372.

Sano, M., Yotsui, Y., Abe, H., & Sasaki, S. (1976). A new technique for the detection of metabolites labelled by the isotope ^{13}C using mass fragmentography. *Biomedical Mass Spectrometry*, *3*, 1–3.

Shinebarger, S. R., Haisch, M., & Matthews, D. E. (2002). Retention of carbon and alteration of expected ^{13}C-tracer enrichments by silylated derivatives using continuous-flow combustion-isotope ratio mass spectrometry. *Analytical Chemistry*, *74*, 6244–6251.

Skarpeli-Liati, M., Turgeon, A., Garr, A. N., Arnold, W. A., Cramer, C. J., & Hofstetter, T. B. (2011). pH-dependent equilibrium isotope fractionation associated with the compound specific nitrogen and carbon isotope analysis of substituted anilines by SPME-GC/IRMS. *Analytical Chemistry*, *83*, 1641–1648.

Styring, A. K., Fraser, R. A., Arbogast, R.-M., Halstead, P., Isaakidou, V., Pearson, J. A., et al. (2015). Refining human palaeodietary reconstruction using amino acid δ^{15}N values of plants, animals and humans. *Journal of Archaeological Science*, *53*, 504–515.

Styring, A. K., Fraser, R. A., Bogaard, A., & Evershed, R. P. (2014). Cereal grain, rachis and pulse seed amino acid δ^{15}N values as indicators of plant nitrogen metabolism. *Phytochemistry*, *97*, 20–29.

Tcherkez, G., Mahe, A., & Hodges, M. (2011). ^{12}C/^{13}C fractionations in plant primary metabolism. *Trends in Plant Science*, *16*, 499–506.

Tea, I., Antheaume, I., Besnard, J., & Robins, R. J. (2010). Determination of the natural abundance δ^{15}N of taurine by gas chromatography-isotope ratio measurement mass spectrometry. *Rapid Communications in Mass Spectrometry*, *24*, 3380–3386.

Tea, I., Ferchaud-Roucher, V., Küster, A., Darmaun, D., & Robins, R. J. (2007). Determination of ^{13}C isotopic enrichment of glutathione and glycine by gas chromatography/combustion/isotope ratio mass spectrometry after formation of the N- or N,S-ethoxycarbonyl methyl ester derivatives. *Rapid Communications in Mass Spectrometry*, *21*, 3245–3252.

Tea, I., Le Guennec, A., Frasquet-Darrieux, M., Julien, M., Romek, K., Antheaume, I., et al. (2013). Simultaneous determination of natural-abundance δ^{15}N values and quantities of individual amino acids in proteins from milk of lactating women and from infant hair using gas chromatography/isotope ratio mass spectrometry. *Rapid Communications in Mass Spectrometry*, *27*, 1345–1353.

Tea, I., Martineau, E., Antheaume, I., Lalande, J., Mauve, C., Gilard, F., et al. (2016). ^{13}C and ^{15}N natural isotope abundance reflects breast cancer cell metabolism. *Scientific Reports*, *6*, Article number 34251.

Thevis, M., Piper, T., Horning, S., Juchelka, D., & Schänzer, W. (2013). Hydrogen isotope ratio mass spectrometry and high-resolution/high-accuracy mass spectrometry in metabolite identification studies: Detecting target compounds for sports drug testing. *Rapid Communications in Mass Spectrometry*, *27*, 1904–1912.

van Dongen, B. E., Schouten, S., & Damsté, J. S. S. (2001). Gas chromatography/combustion/isotope-ratio-monitoring mass spectrometric analysis of methylboronic derivatives

of monosaccharides: A new method for determining natural ^{13}C abundances of carbohydrates. *Rapid Communications in Mass Spectrometry*, *15*, 496–500.

Verbeke, K., Ferchaud-Roucher, V., Preston, T., Small, A. C., Henckaerts, L., Krempf, M., et al. (2010). Influence of the type of indigestible carbohydrate on plasma and urine short-chain fatty acid profiles in healthy human volunteers. *European Journal of Clinical Nutrition*, *64*, 678–684.

Wang, J., Yang, R., Yang, W., Liu, X., Xing, Y., & Xu, Y. (2014). IRMS detection of testosterone manipulated with ^{13}C labeled standards in human urine by removing the labeled ^{13}C. *Analytica Chimica Acta*, *852*, 146–152.

Webb, E. C., Honch, N. V., Dunn, P. J. H., Eriksson, G., Lidén, K., & Evershed, R. P. (2015). Compound-specific amino acid isotopic proxies for detecting freshwater resource consumption. *Journal of Archaeological Science*, *63*, 104–114.

Zech, M., Saurer, M., Tuthorn, M., Rinne, K., Werner, R. A., Siegwolf, R., et al. (2013). A novel methodological approach for $\delta^{18}O$ analysis of sugars using gas chromatography-pyrolysis-isotope ratio mass spectrometry. *Isotopes in Environmental and Health Studies*, *49*, 492–502.

Zhang, H., Wang, Z., & Liu, O. (2015). Development and validation of a GC–FID method for quantitative analysis of oleic acid and related fatty acids. *Journal of Pharmaceutical Analysis*, *5*, 223–230.

Zhou, Y., Grice, K., Stuart-Williams, H., Hocart, C. H., Gessler, A., & Farquhar, G. D. (2016). Hydrogen isotopic differences between C_3 and C_4 land plant lipids: Consequences of compartmentation in C_4 photosynthetic chemistry and C_3 photorespiration. *Plant, Cell & Environment*, *39*, 2676–2690.